

Mathematical model to analyze phosphor layer heat transfer of an LED system

Indika U. Perera and Nadarajah Narendran*
Lighting Research Center, Rensselaer Polytechnic Institute, Troy, NY 12180

ABSTRACT

This study investigated the capability of a mathematical model in estimating the phosphor layer heat transfer of an LED system. The focus was on determining the temperature distribution based on light propagation in the phosphor layer. The mathematical model was built upon past work by Kang et al. and solved numerically with heat generation and transfer incorporated into the model. The model light propagation and heat generation was compared with past research and then used to simulate an experimental study in order to evaluate the solution from the present model and compare it with the temperature measurements of the experimental study. The solution to the temperature distribution using the mathematical model had good agreement with the experimentally measured temperature values using an IR thermal imaging camera. Then the model was used to predict the temperature distribution in the phosphor layer under different heat transfer conditions to provide insight that is difficult to observe in experimental studies due to practical limitations.

Keywords: light-emitting diode, heat transfer, mathematical model, phosphor layer temperature, phosphor layer heat generation, IR thermography

1. INTRODUCTION

In a white light-emitting diode (LED) system, short-wavelength visible radiation emitted by a semiconductor chip is partially down-converted into broadband, long-wavelength visible radiation using a phosphor material^[1]. The combination radiation is perceived by the human visual system as “white” light^[2]. The energy conversion processes involved in creating this white light have inherent conversion inefficiencies as well as extraction inefficiencies of generated photons at both the LED chip and the white LED package, leading to the generation of heat. The heat generated in an LED package or a system therefore can be broadly categorized into two parts, namely the heat generated in the LED chip and the heat generated in the phosphor layer.

The heat generated in the LED chip is mainly due to the conversion inefficiencies of the semiconductor chip in converting electrical energy into short-wavelength visible radiation. The LED chip performance and the effect of temperature have been studied extensively and performance improvements have been reported with adequate heat dissipation via heat sinks^[3].

The heat generated in the phosphor material is due to the losses caused by a deficit in the quantum efficiency of the phosphor material and the Stokes shift loss. In addition to these losses, photons not extracted from the LED and the package are absorbed and lead to heat generation. The generated heat and subsequent increase in operating temperature cause LED system performance to be negatively affected^[4]. The heat generation by the phosphor within the binding medium, hereinafter termed the phosphor layer, has become a focus at present due to research findings reporting phosphor layer operating temperatures being higher than LED chip junction temperature^[5]. Phosphor quenching and binding medium degradation are both directly related to the phosphor layer temperature.

Due to limitations in experimental methods, devices, and equipment, measuring the temperature distribution within the phosphor layer has been difficult. The absorption of visible radiation (emitted by the LED chip and the phosphor layer) at the temperature measuring devices and physical limitations of placing the devices in the phosphor layer (to ensure light propagation is not obstructed) are some of the limitations in experimentally measuring temperature profiles^[6]. Therefore, the objective of the present study was to use a mathematical model to numerically simulate the light propagation and heat generation in the phosphor layer and thereby predict the phosphor layer temperature profile.

*Corresponding author: +1 (518) 687-7100; narenn2@rpi.edu; <http://www.lrc.rpi.edu/programs/solidstate>

2. METHODOLOGY AND MATHEMATICAL MODEL

A number of past studies have investigated the phosphor layer heat generation and temperature by assuming modeling volumetric heat generation quantities for the phosphor layer^{[7],[8]}, while others quantified the heat generation based on light propagation through the phosphor layer^[9]. Kang et al. modeled the light propagation in a phosphor layer with a one-dimensional (1D) analytical model^[10] while Huang et al. modeled light propagation as well as heat generation in the phosphor layer with a 1D analytical model^[9]. Both these models used the energy balance equation in modeling the light propagation and the heat generation in the phosphor layer. The model introduced by Kang et al. was used in the present study due to simplicity where it only considered absorption in the phosphor layer and did not consider light scattering by the phosphor particles. The basic derivation of the present mathematical model is presented in Figure 1.

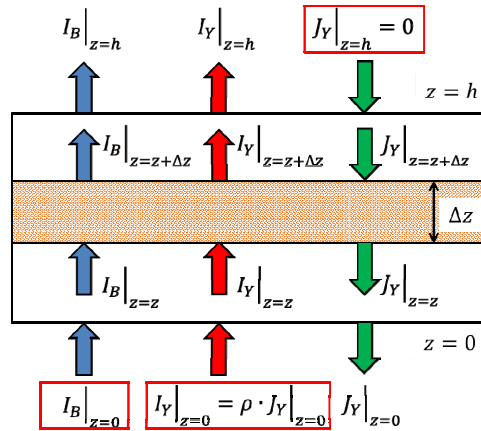


Figure 1. Schematic diagram of the 1D light propagation through the phosphor layer with boundary conditions

Figure 1 illustrates the schematic diagram of a phosphor layer of h thickness in the z -direction where the surface at $z = 0$ is facing the LED chips. The narrowband blue light emitted from these LED chips incident on the phosphor layer is partially absorbed by the phosphor layer. This absorption loss of blue light as it propagates through the phosphor layer follows Lambert-Beer's law, where the irradiance of the transmitted light is proportional to the incident blue light irradiance. The blue light irradiance propagating in the positive z -direction is denoted as I_B in Figure 1. Part of this absorbed irradiance is down-converted and re-emitted by the phosphor particles isotropically, implying that half of the down-converted yellow light propagates in the positive z -direction while the other half propagates in the negative z -direction. The propagation irradiance in the positive z -direction is denoted as I_Y while the propagation irradiance in the negative z -direction is denoted as J_Y . In the present model, light scattering, both blue light and yellow light, is considered to be minimal. Considering the infinitesimally thin sub-layer of Δz thickness, the following differential equations can be written:

$$\frac{dI_B}{dz} = -\alpha_B \cdot I_B \quad (1)$$

$$\frac{dI_Y}{dz} = -\alpha_Y \cdot I_Y + \frac{1}{2} \cdot \eta \cdot \alpha_B \cdot I_B \quad (2)$$

$$\frac{dJ_Y}{dz} = \alpha_Y \cdot J_Y - \frac{1}{2} \cdot \eta \cdot \alpha_B \cdot I_B \quad (3)$$

Where α_B and α_Y are absorption coefficients per unit length reduction in irradiance as blue and yellow light propagate in the phosphor layer while η denotes total conversion efficiency of the phosphor from blue to yellow. The quantity $\eta \cdot \alpha_B$ is defined as the conversion coefficient of the phosphor layer in converting blue light to yellow light per unit length of propagation by Kang et al. in their study^[10]. In order to solve the differential equations above the following boundary conditions were used:

$$I_B|_{z=0} = I_{B0} \quad (4)$$

$$I_Y|_{z=0} = \rho \cdot J_Y|_{z=0} \quad (5)$$

$$J_Y|_{z=h} = 0 \quad (6)$$

Where I_{B0} is the irradiance emitted by the LED chips on the phosphor layer surface closest to the LEDs while ρ is the yellow light reflectance from the LED and LED mounting surfaces back towards the phosphor layer. Due to the assumption made with regards to the blue light scattering being negligible, it is also assumed that there is no blue reflected component off the LED and LED mounting surfaces towards the phosphor layer. In the present study, these differential equations were solved numerically to satisfy equation (5) using an iterative scheme.

The heat generation was modeled based on the assumption that absorption of light in the phosphor layer caused heat generation based on the energy balance equation. Therefore, considering the infinitesimally small sub-layer of Δz in Figure 1, the heat generation rate in that layer can be written as:

$$\dot{E}_g(z) = \alpha_B \cdot (1 - \eta) \cdot I_B + \alpha_Y \cdot (I_Y + J_Y) \quad (7)$$

In order to evaluate the temperature profile in the phosphor layer, a 2D axisymmetric heat transfer model with heat generation as per the volumetric heat generation described by equation (7) was used. The axisymmetry was used based on the geometry of the phosphor layer as it will be explained in the subsequent section. The general 2D axisymmetric heat transfer equation used is listed below.

$$\frac{\partial^2 T(r, z)}{\partial r^2} + \frac{1}{r} \frac{\partial T(r, z)}{\partial r} + \frac{\partial^2 T(r, z)}{\partial z^2} + \frac{\dot{E}_g(z)}{k} = 0 \quad (8)$$

In solving the heat equation listed above, four boundary conditions (the axisymmetry of the phosphor layer and convection boundary conditions on the other three sides) were used based on the geometry and experimental conditions as explained below.

3. EXPERIMENT

An experiment was conducted to measure the temperature distribution on the emitting surface of a phosphor layer. Figure 2 illustrates the experimental setup used for the temperature measurement. An array of blue LEDs was used in a reflector cup with a temperature-controlled heat sink. A phosphor layer was deposited onto machined heat sink plates with high thermal conductivity similar to previous work^[11]. A nitride phosphor used in this study generated a large amount of heat due to higher conversion losses. A thermal imaging camera with a wavelength sensitivity range of 7.5-14 μm was used to measure the phosphor layer surface temperature. An enclosure was used to minimize the IR reflections' effect on temperature measurement.

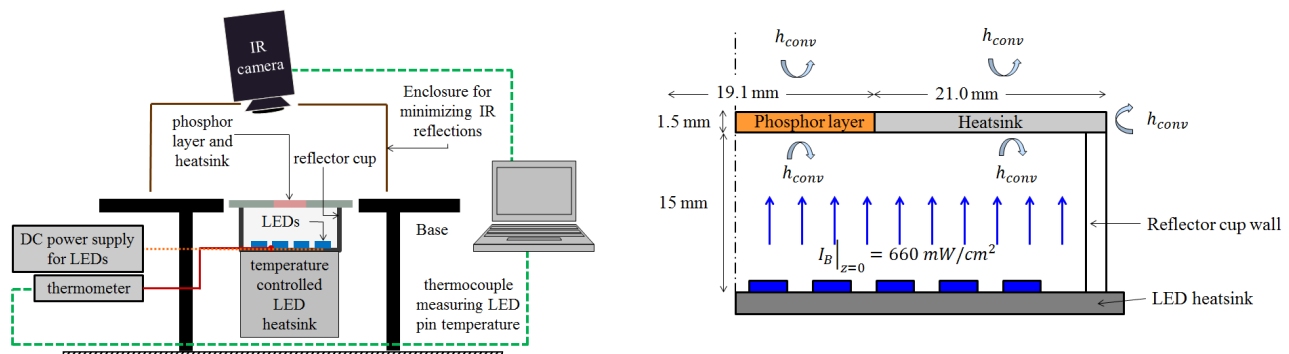


Figure 2. Schematic diagram of the experimental setup (left) and phosphor layer heat sink with LEDs in reflector cup arrangement and experimental conditions (right)

The phosphor blue light absorption coefficient and red light absorption coefficient were calculated from the transmission and reflection components of the light using a double integrating sphere measurement setup. The double integrating sphere experimental apparatus used was similar to the apparatus used in past research^{[12],[13]} while the calculations of the absorption coefficients were based on Sardar et al.'s work^[13]. The conversion efficiency of the phosphor was calculated from spectral power distributions recorded using an integrating sphere measurement system. The phosphor characterization was done for the same phosphor weight fraction as the phosphor layers deposited in the phosphor heat sink plates. The blue light irradiance on the phosphor layer surface closest to the LEDs was measured in the experimental setup and used in the light propagation model as one of the boundary conditions.

4. PRELIMINARY MODEL VALIDATION

The phosphor parameters were adopted from Kang et al.'s experimental data and linear approximations were used in describing the dependence of α_B , α_Y , and $\eta \cdot \alpha_B$ on volume fraction of phosphor, as stated by Kang et al. in their study^[10].

In order to validate the present model's numerical solution, Kang et al.'s results from their analytical model were used and the comparison is illustrated in Figure 3. The blue irradiance and the yellow irradiance exiting the surface at $z = h$ is the total irradiance of the phosphor layer. This total irradiance is normalized using the blue light irradiance on the surface at $z = 0$ emitted by the blue LED chips. The discrepancy between Kang et al.'s analytic solution and the numerical solution presented by the present study was due to the linear equations used in describing the relationship of α_B , α_Y , and $\eta \cdot \alpha_B$ on volume fraction of phosphor in the phosphor layer. In order to validate this, the analytic model used by Kang et al. in the original study was solved using the linear relationship of α_B , α_Y , and $\eta \cdot \alpha_B$ on volume fraction of phosphor in the phosphor layer and plotted on the same Figure 3 (\circ indicating the analytical model for 30 μm phosphor layer and \square indicating the analytic model for 150 μm phosphor layer). This provided validation of the mathematical model used in the present study by matching results of Kang et al. for light propagation.

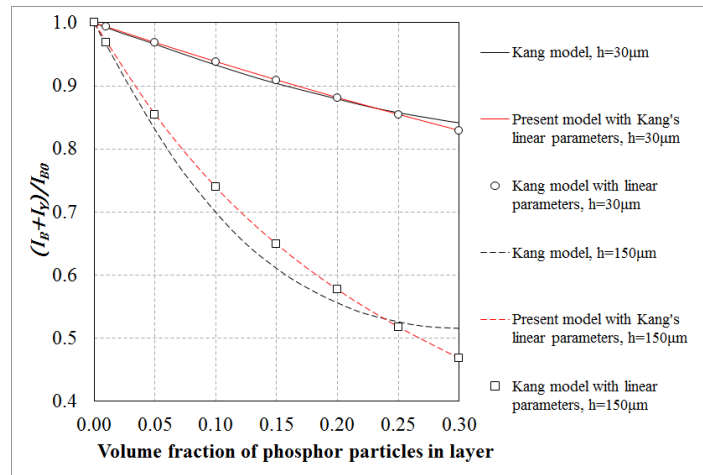


Figure 3. Dependence of normalized total irradiance of light exiting the phosphor layer on volume fraction of phosphor particles in the phosphor layer. Kang et al.'s analytical solution compared with present model numerical solution.

In order to validate the heat generation of the present model, Huang et al.'s model^[9] was used which was developed in an identical manner to Kang et al.'s model except Huang et al.'s model incorporates light scattering by phosphor particles.

$$\frac{d(E_t/E_{B_in})}{d(z/h)} = \frac{(1 - \eta) \ln \left[1 + \frac{2}{\eta(1 + \gamma) E_{B_out}/E_{Y_out}} \right]}{\left[1 + \frac{2}{\eta(1 + \gamma) E_{B_out}/E_{Y_out}} \right]^{z/h}} \quad (8)$$

The heat generation in Huang et al.'s model used equation (8), which gives the normalized volumetric heat power on the left side of the equation as a function of the phosphor conversion efficiency (η), blue to yellow light radiant flux density ratio exiting the phosphor layer furthest from the LEDs ($E_{B,out}/E_{Y,out}$), reflectance of yellow light off the LEDs and LED mounting surface (γ), the blue light irradiance on the surface closest to the LEDs ($E_{B,in}$), and the thickness of the phosphor layer (h) in the z -direction^[9].

Figure 4 shows the normalized volumetric heat generation calculated from Huang et al.'s analytical model and the present model. The figure below shows for two blue to yellow irradiance ratios (IB/IY=0.12 and 0.37) the normalized volumetric heat generation for the two models as the normalized distance through the phosphor layer is increased. The present model over-predicts the normalized heat generation compared with Huang et al.'s model as the distance increases from the surface at $z = 0$ closest to the LEDs by a maximum of ~10% at the surface $z = h$. We believe this is because the light propagation model used in the present study did not take into account light scattering by the phosphor particles, while Huang's analytical model incorporates scattering of the blue and the yellow light off phosphor particles.

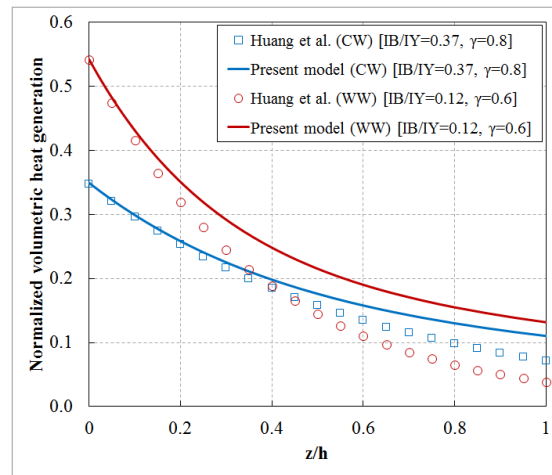


Figure 4. Normalized volumetric heat generation against normalized distance in the z -direction through the phosphor layer using Huang et al.'s analytical model and the present model.

Since Huang et al.'s study did not have experimental validation of the heat generation model, the present study used the temperature profile measured in the experimental setup that was described earlier in order to validate the present model's heat generation. The phosphor layer embedded in the heat sink was modeled as described in the previous section with surface boundary conditions emulating the experimental conditions.

5. RESULTS AND DISCUSSION

The measured temperature profile on the phosphor layer emitting surface is shown below in Figure 5.

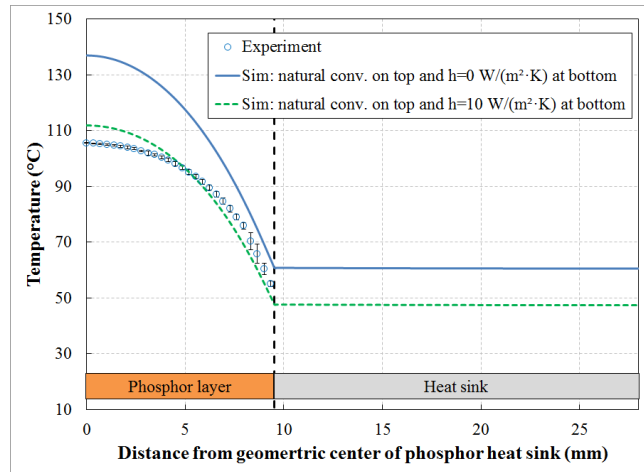


Figure 5. Experimental measured temperature profile on the phosphor layer surface with numerical solution temperature profile using the present model.

The vertical discontinuous line indicates the interface between the phosphor layer and the heat sink material. The temperature decreased as the distance from the geometric center increased in the phosphor layer due to the axisymmetric boundary condition on the left and the convective boundary conditions on the right. The error bars on the experimental data points indicate the standard deviation of multiple measurements in different radial directions. The two simulation results plotted on the same figure illustrate two different boundary conditions used at the phosphor layer surface closest to the LEDs. The blue continuous line is for the insulated boundary condition while the green discontinuous line is for a convective coefficient of $10 \text{ W}/(\text{m}^2 \cdot \text{K})$, which is a reasonable number for the reflective cavity dimensions. The simulation results agreed with the experimental results to within $\sim 5\text{-}10^\circ\text{C}$.

A number of simulations were conducted to understand the temperature dependence on the heat transfer in the problem explained above. The effect of thermal conductivity of the phosphor layer heat sink was evaluated using the model and the results are shown in Figure 6 by fixing the convective heat transfer to be driven by natural convection on top of the phosphor layer and insulated at the bottom surface. The phosphor layer thermal conductivity and other parameters were held constant. The increase in thermal conductivity of the heat sink material reduced the phosphor layer temperature provided the thermal conductivity was higher than $10 \text{ W}/(\text{m} \cdot \text{K})$ and any further increase reduces the temperature marginally in both radial and axial directions.

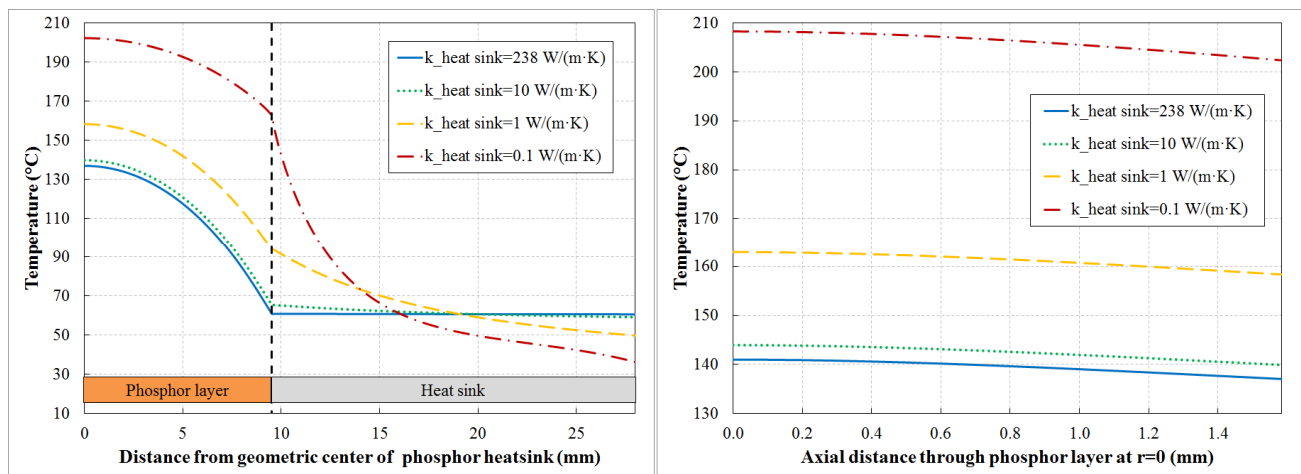


Figure 6. Phosphor layer temperature profile: in the radial direction on the surface farthest from the LEDs (left) and in the axial direction through the phosphor layer at $r=0$ (right).

Similarly, simulations were conducted with varying the heat convection on the two phosphor layer surfaces closest and farthest from the LEDs, with increasing convection on either surface reducing the temperature in the radial direction while the temperature gradient further reduced in the axial direction, as seen in previous experimental work^[14]. In a couple of simulations, where the convective coefficient was relatively high (e.g., 20 W/(m²·K)), the center of the phosphor layer exhibited the highest temperature. This temperature was only a marginal increase (e.g., by ~1-2°C) over the temperatures at $z = 0$ and $z = h$ surfaces.

6. SUMMARY

The mathematical model was able to predict the trend of the temperature profile in the phosphor layer, although there were absolute temperature discrepancies. The numerical results illustrated that temperature gradient through the phosphor layer was minimal (~5°C), even with low thermal conductivity of the phosphor layer binding material. Incorporation of light scattering to the present model is an important step in the future work, which will enable the model to predict the absolute temperature distribution in the phosphor layer more accurately. In order to predict the light propagation and subsequent heat generation using mathematical models, the phosphor characterization and model assumptions are of paramount importance.

ACKNOWLEDGMENTS

We would like to acknowledge the financial support of the Lighting Research Center at Rensselaer Polytechnic Institute, Henkel, and the Besal Lighting Education Fund provided by Acuity Brands Lighting; and the contribution and support of Yi-wei Liu, Yiting Zhu, Jean Paul Freyssinier, Martin Overington, Howard Ohlhous, and Jennifer Taylor at the LRC.

REFERENCES

- [1] Nakamura, S., Mukai, T., and Senoh, M., "Candela-class high-brightness InGaN/AlGaIn double heterostructure blue-light emitting diodes," *Appl. Phys. Lett.* 64, 1687–1689 (1994); doi: 10.1063/1.111832.
- [2] Narendran, N., Gu, Y., Freyssinier-Nova, J., and Zhu, Y., "Extracting phosphor-scattered photons to improve white LED efficiency," *Physica Status Solidi (A)* 202(6), R60–R62 (2005).
- [3] Arik, M., Becker, C., Weaver, S., and Petroski, J., "Thermal management of LEDs: Package to system," *Proc. SPIE* 5187, 64–75 (2004); doi: 10.1117/12.512731.
- [4] Lin, C.-C. and Liu, R.-S., "Advances in phosphors for light-emitting diodes," *J. Phys. Chem. Lett.* 2(11), 1268–1277 (2011); doi: 10.1021/jz2002452.
- [5] Yan, B., Tran, N. T., You, J.-P., and Shi, F. G., "Can junction temperature alone characterize thermal performance of white LED emitters?," *IEEE Photonics Technol. Lett.* 23(9), 555–557 (2011); doi: 10.1109/LPT.2011.2115997.
- [6] Perera, I. U., Narendran, N., and Liu, Y., "Accurate measurement of LED lens surface temperature," *Proc. SPIE* 8835, 883506 (2013); doi: 10.1117/12.2023091.
- [7] Arik, M., Weaver, S., Backer, C., Hsing, M., and Srivastav, A., "Effects of localized heat generations due to the color conversion in phosphor particles and layers of high brightness light emitting diodes," *Advances in Electronic Packaging*, 2003 International Electronic Packaging Technical Conference and Exhibition, Vol. 3, 613–619 (2003).
- [8] Luo, X., Fu, X., Chen, F., and Zheng, H., "Phosphor self-heating in phosphor converted light emitting diode packaging," *J. Heat Mass Transfer* 58, 276–281 (2013); doi: 10.1016/j.jheatmasstransfer.2012.11.056.
- [9] Huang, M. and Yang, L., "Heat generation by the phosphor layer of high-power white LED emitters," *IEEE Photonics Technol. Lett.* 25(4), 1317–1320 (2013); doi: 10.1109/LPT.2013.2263375.
- [10] Kang, D.-Y., Wu, E., and Wang, D.-M., "Modeling white light-emitting diodes with phosphor layers," *Appl. Phys. Lett.* 89, 231102-1–3 (2006); doi: 10.1063/1.2400111.
- [11] Perera, I. U. and Narendran, N., "Thermal management of the remote phosphor layer in LED systems," *Proc. SPIE* 8835, 883504 (2013); doi: 10.1117/12.2023094.
- [12] Zhu, Y., [Investigation of the optical properties of YAG:Ce phosphor at different wavelengths], Master's Thesis, Lighting Research Center, Rensselaer Polytechnic Institute, Troy, NY (2006).
- [13] Sardar, D. K., Yust, B. G., Barrera, F. J., Mimun, L. C., and Tsin, A. T. C., "Optical absorption and scattering of bovine cornea, lens and retina in the visible region," *Laser Med. Sci.* 24(6), 837–847 (2009); doi:10.1007/s10103-009-0677-0.
- [14] Perera, I. U. and Narendran, N., "Understanding heat dissipation of a remote phosphor layer in an LED system," *ITHERM 2014: The 14th IEEE Intersociety Conference on Thermal and Thermomechanical Phenomena in Electronic Systems*, Lake Buena Vista, FL, May 27–30, 2014, pp. 186–192 (2014).